

# Selective dysregulation of ROCK2 activity promotes aberrant transcriptional networks in ABC diffuse large B cell lymphoma

Edd Ricker<sup>1,2</sup>, Akanksha Verma<sup>3</sup>, Rossella Marullo<sup>4</sup>, Sanjay Gupta<sup>1</sup>, Chao Ye<sup>1</sup>,  
Tania Pannellini<sup>5</sup>, Michela Manni<sup>1</sup>, Wayne Tam<sup>6</sup>, Giorgio Inghirami<sup>6</sup>, Olivier Elemento<sup>3</sup>,  
Leandro Cerchietti<sup>4</sup>, and Alessandra B. Pernis<sup>\*1, 2, 7, 8</sup>

<sup>1</sup>Autoimmunity and Inflammation Program, Hospital for Special Surgery, NY, NY, USA

<sup>2</sup>Graduate Program in Immunology and Microbial Pathogenesis, Weill Cornell Graduate School of Medical Sciences, NY, NY, USA

<sup>3</sup>Caryl and Israel Englander Institute for Precision Medicine, Department of Physiology and Biophysics, Weill Cornell Medicine, NY, NY, USA

<sup>4</sup>Hematology and Oncology Division, Weill Cornell Medicine, NY, NY, USA

<sup>5</sup>Research Division and Precision Medicine Laboratory, Hospital for Special Surgery, NY, NY, USA

<sup>6</sup>Department of Pathology and Laboratory Medicine, Weill Cornell Medicine, NY, NY, USA

<sup>7</sup>David Z. Rosensweig Genomics Research Center, Hospital for Special Surgery, NY, NY, USA

<sup>8</sup>Department of Medicine, Weill Cornell Medicine, NY, NY, USA

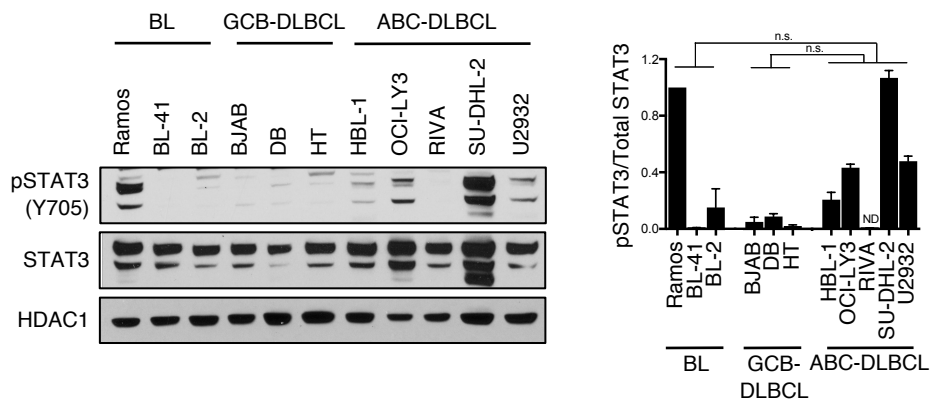
## Correspondence:

\*Alessandra B. Pernis

Autoimmunity and Inflammation Program, Hospital for Special Surgery, 535 East 70th Street, New York, NY 10021, USA. Tel: 212-206-1612. E-mail: [pernisa@hss.edu](mailto:pernisa@hss.edu)

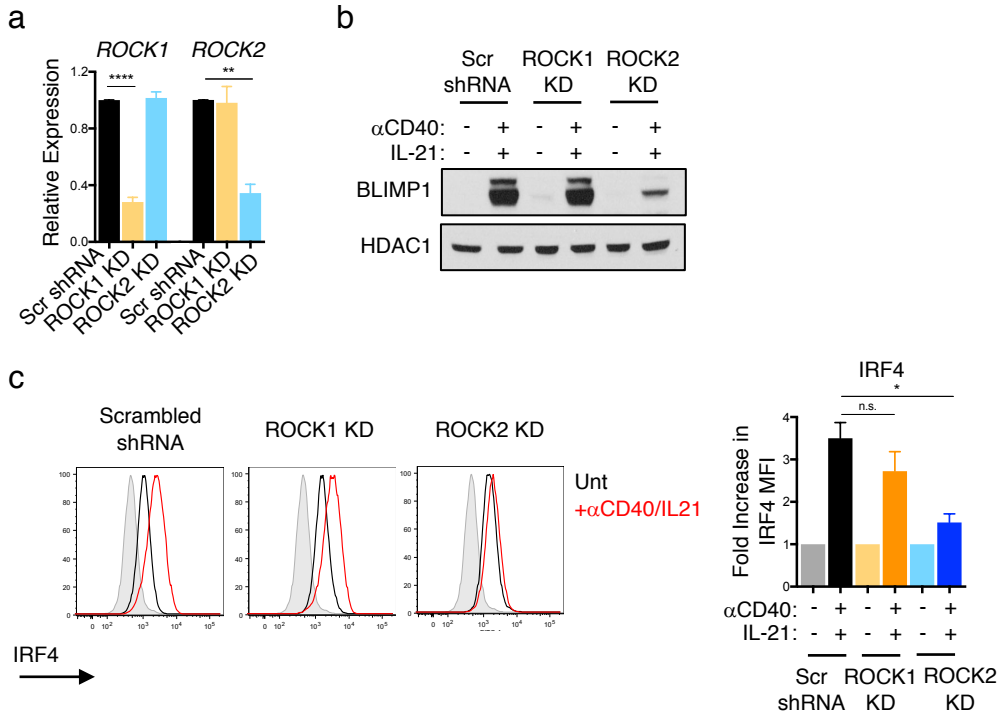
Figure S1.

a



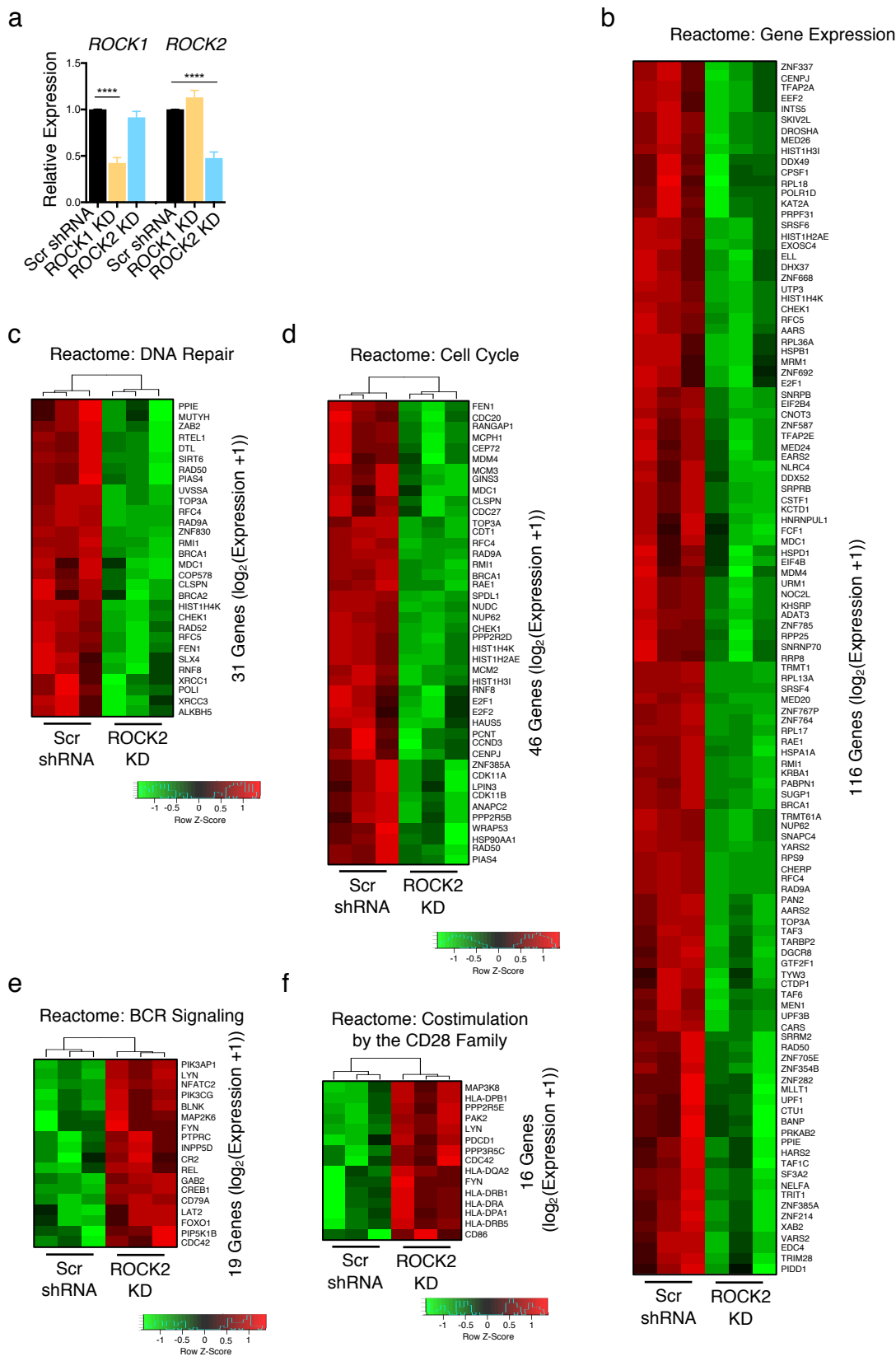
**Figure S1. (A)** Representative immunoblot and quantifications of phosphorylated STAT3 (pSTAT3; Y705), total STAT3, and HDAC1 as a loading control from nuclear extracts of BL (Ramos, BL-41, BL-2), GCB-DLBCL (BJAB, DB, HT), and ABC-DLBCL (HBL-1, OCI-LY3, RIVA, SU-DHL-2, U2932) cell lines. Quantifications are calculated as the densitometry ratio between pSTAT3 to total STAT3 (mean  $\pm$  SEM,  $n=2$ ;  $p$ -value by 1-way ANOVA followed by Tukey's multiple comparisons test). ns  $p>0.05$ .

Figure S2.



**Figure S2. (A)** Pooled RT-qPCR analysis of *ROCK1* and *ROCK2* transcripts relative to 28S in Ramos cells after stable lentiviral infection with shRNA constructs as in Fig. 3 (mean  $\pm$  SEM;  $n=3$ ; p-value by 1-way ANOVA followed by Dunnett's multiple comparisons test). **(B-C)** Stable Ramos ROCK1 KD, ROCK2 KD, and scrambled shRNA control cells were left untreated or stimulated for 6hr with  $\alpha$ CD40 and IL-21. **(B)** Representative immunoblot of BLIMP1 and HDAC1 as a loading control. Immunoblot representative of 2 independent experiments. **(C)** Representative histograms and quantifications of IRF4 expression (mean  $\pm$  SEM;  $n=2$ ; p-value by 1-way ANOVA followed by Dunnett's multiple comparisons test). \* $p<0.05$ , \*\* $p<0.01$ , \*\*\* $p<0.001$ , \*\*\*\* $p<0.0001$ .

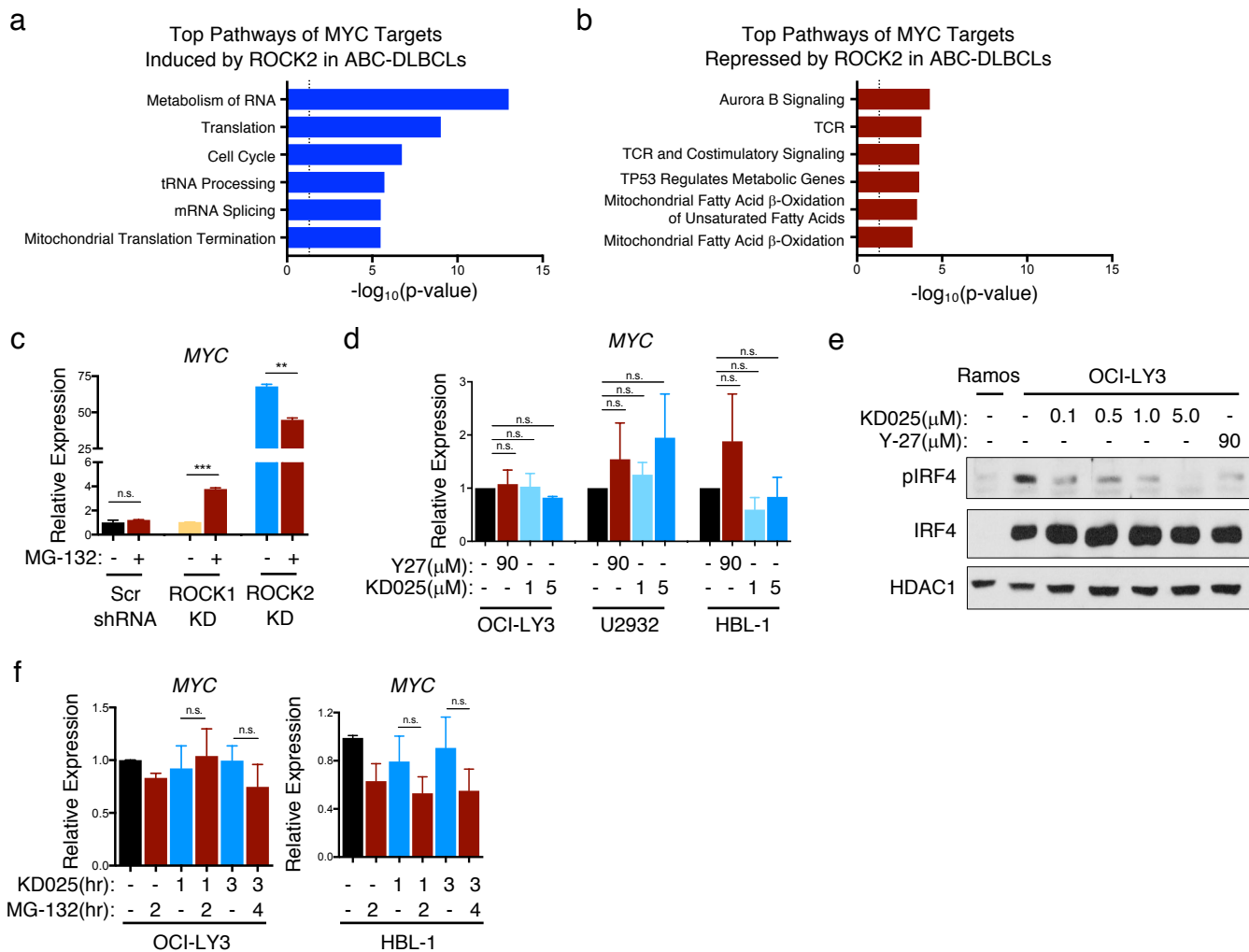
Figure S3.





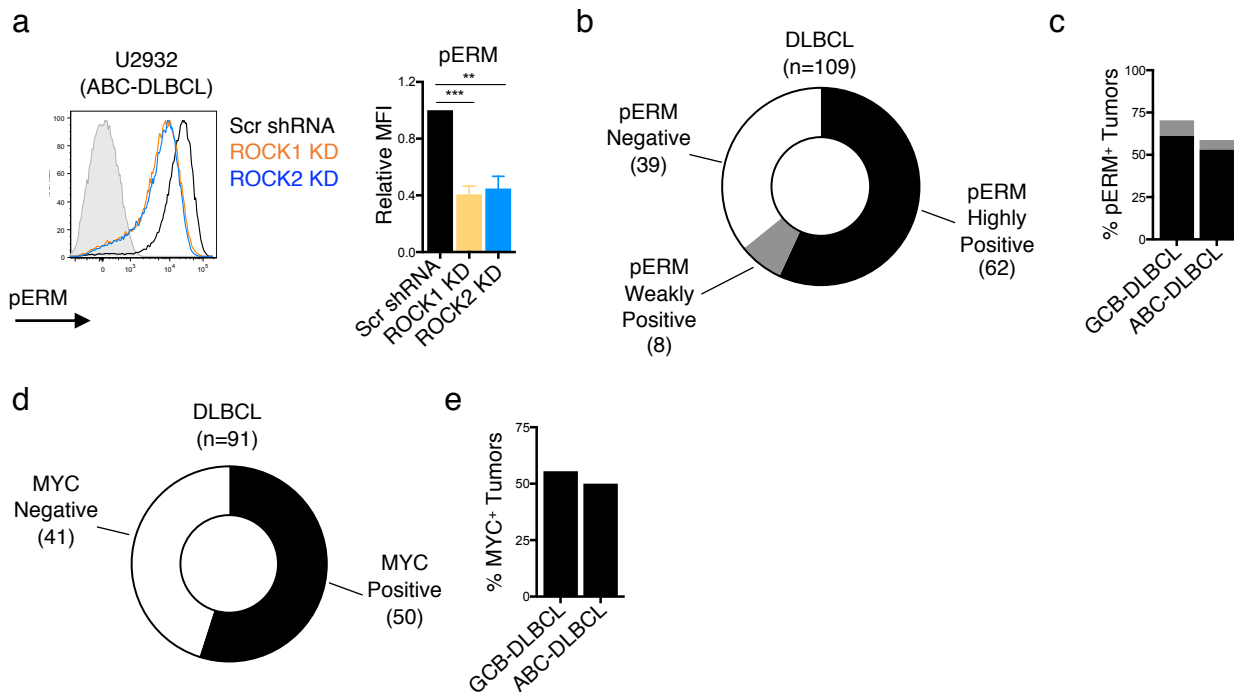
**Figure S3. (A)** Pooled RT-qPCR analysis of *ROCK1* and *ROCK2* expression relative to 28S in U2932 cells following lentiviral infections as in Fig. 4 (mean +/- SEM;  $n=5$ ; p-value by 1-way ANOVA followed by Dunnett's multiple comparisons test). **(B-F)** Heat map depictions of differentially expressed genes in the U2932 ROCK2 KD cells compared to the scrambled shRNA control cells composing the gene expression (B), DNA repair (C), cell cycle (D), BCR signaling (E), and costimulation by the CD28 family (F) pathways from the over-representation pathway analysis in Fig. 4C-D. \* $p<0.05$ , \*\* $p<0.01$ , \*\*\* $p<0.001$ , \*\*\*\* $p<0.0001$ .

Figure S4.



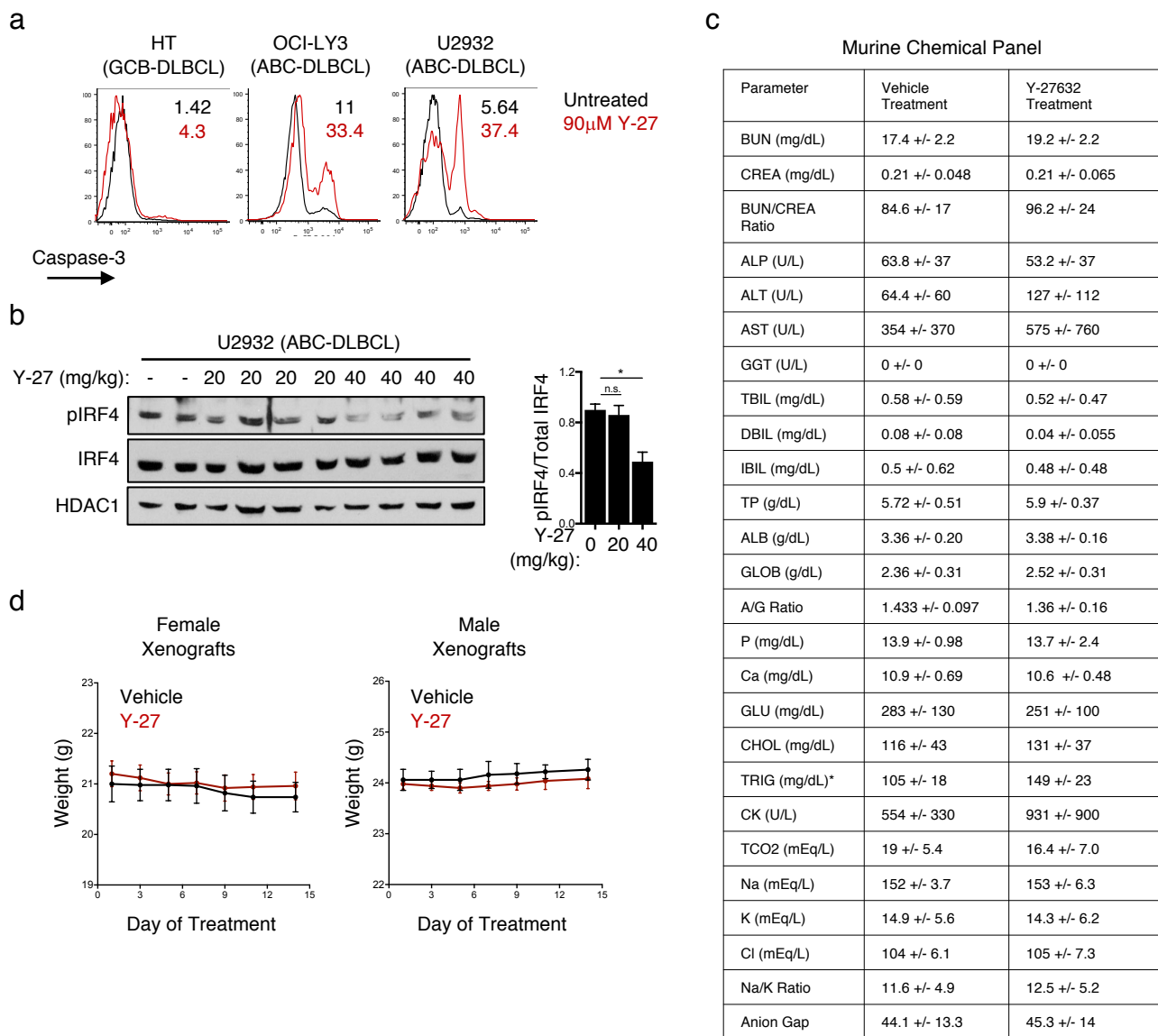
**Figure S4. (A-B)** Plots showing the  $-\log_{10}(p\text{-value})$  values for the top over-represented pathways from the genes representing the ROCK2-induced (A) or the ROCK2-repressed (B) MYC targets in U2932. Dotted lines indicate significance cutoffs at  $p=0.05$ . **(C)** Representative RT-qPCR analysis for MYC transcripts compared to 28S from the experiment in Fig. 5C. Data representative of 2 independent experiments (mean +/- SD; p-value by unpaired two-tailed t-test). **(D)** Pooled RT-qPCR analysis of MYC (mean +/- SEM;  $n=3$ ; p-value by 1-way ANOVA followed by Dunnett's multiple comparisons test). **(E)** Representative immunoblot of pIRF4, total IRF4, and HDAC1 in OCI-LY3 cells treated for 6hr with Y-27 or KD025. Data representative of 2 independent experiments. **(F)** Pooled RT-qPCR analysis of MYC transcripts relative to 28S from the experiment in Fig. 5G (mean +/- SEM;  $n=3$ ; p-value by unpaired two-tailed t-tests). \* $p<0.05$ , \*\* $p<0.01$ , \*\*\* $p<0.001$ , \*\*\*\* $p<0.0001$ .

Figure S5.



**Figure S5. (A)** Representative histogram and quantifications of pERM expression in U2932 cells following knockdown of ROCK1 (*orange*), ROCK2 (*blue*), or following infection with a scrambled shRNA control construct (*black*) (mean +/- SEM;  $n=3$ ;  $p$ -value by 1-way ANOVA followed by Dunnett's multiple comparisons test). **(B)** Plot showing the fraction of highly positive, weakly positive, and negative pERM levels in the total DLBCL cases from Fig. 5H. **(C)** Plot showing the frequency of pERM highly positive (*black*) and weakly positive (*grey*) tumors among GCB- and ABC-DLBCL cases from Fig. 5H. **(D)** Plot showing the frequency of MYC-positive tumors of total DLBCL cases from Fig. 5I. **(E)** Plot showing the frequency of MYC-positive tumors among GCB- and ABC-DLBCL cases from Fig. 5I. \* $p<0.05$ , \*\* $p<0.01$ , \*\*\* $p<0.001$ , \*\*\*\* $p<0.0001$ .

Figure S6.



**Figure S6. (A)** Representative histograms of active cleaved caspase-3 in DLBCL cells either left untreated (*black*) or following 24hr treatment with 90 $\mu$ M Y-27 (*red*). Data representative of 3 independent experiments per cell line. **(B-C)** U2932 and HT cells were established as subcutaneous tumors in immunodeficient NSG mice as in Fig. 6E-F. **(B)** Immunoblot analysis and quantifications of phosphorylated IRF4 at S446/S447 (pIRF4), total IRF4, and HDAC1 as a loading control from nuclear extracts of U2932 xenografts treated with 20-40mg/kg Y-27 for 24hr by intraperitoneal injection (mean +/- SEM; p-value by 1-way ANOVA followed by Dunnett's multiple comparisons test). **(C)** Table showing the results of a biochemistry panel on the serum from 5 vehicle-treated and 5 Y-27-treated xenografts collected at the termination of the experiment from Fig. 6E-F (mean +/- SD). **(D)** Weight of tumor-implanted female and male mice following treatment with either PBS (vehicle) or Y-27 as in Fig. 6E-F. Data pooled from 8-10 mice per treatment condition per cell line. \*p<0.05, \*\*p<0.01, \*\*\*p<0.001, \*\*\*\*p<0.0001.

# Full Uncut Gels:

## Figure 1A

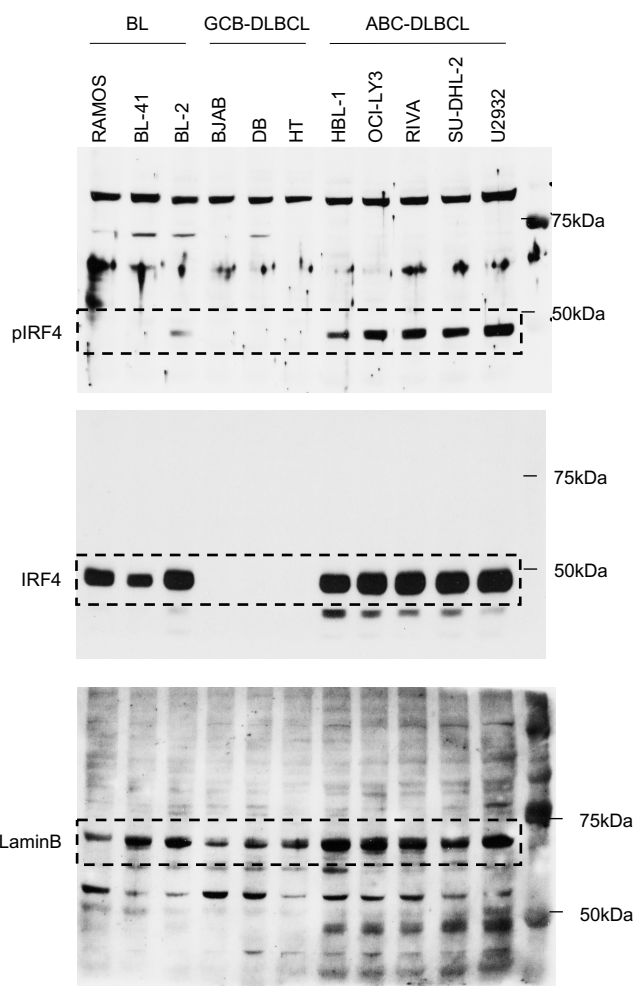
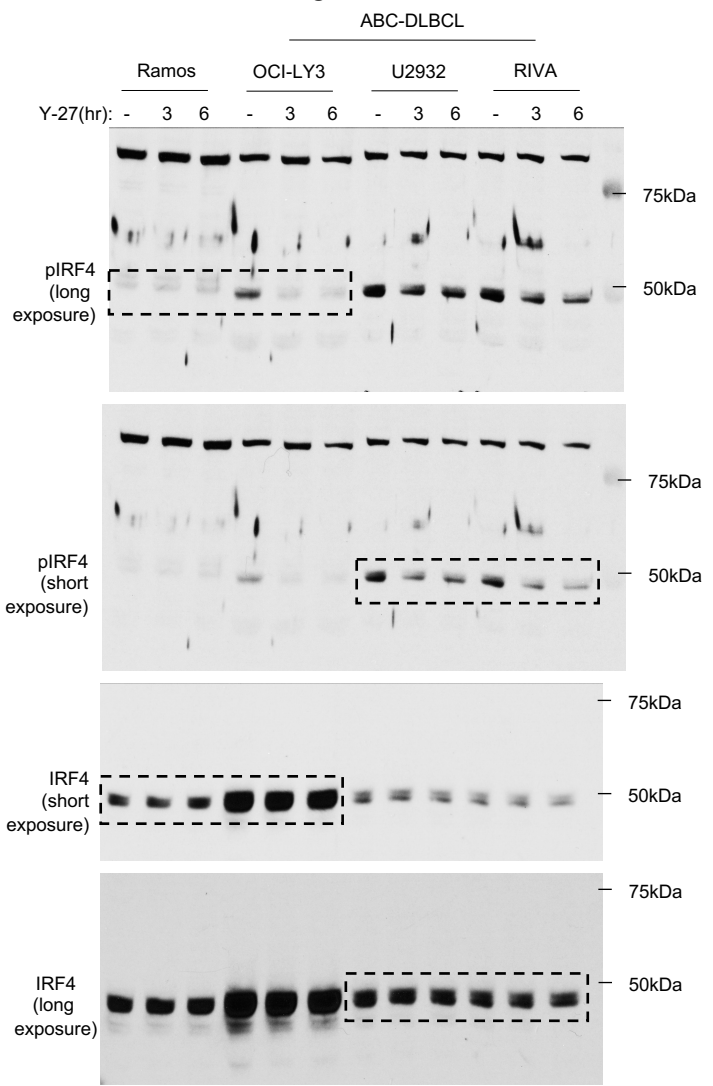


## Figure 1B



# Full Uncut Gels:

## Figure 1D

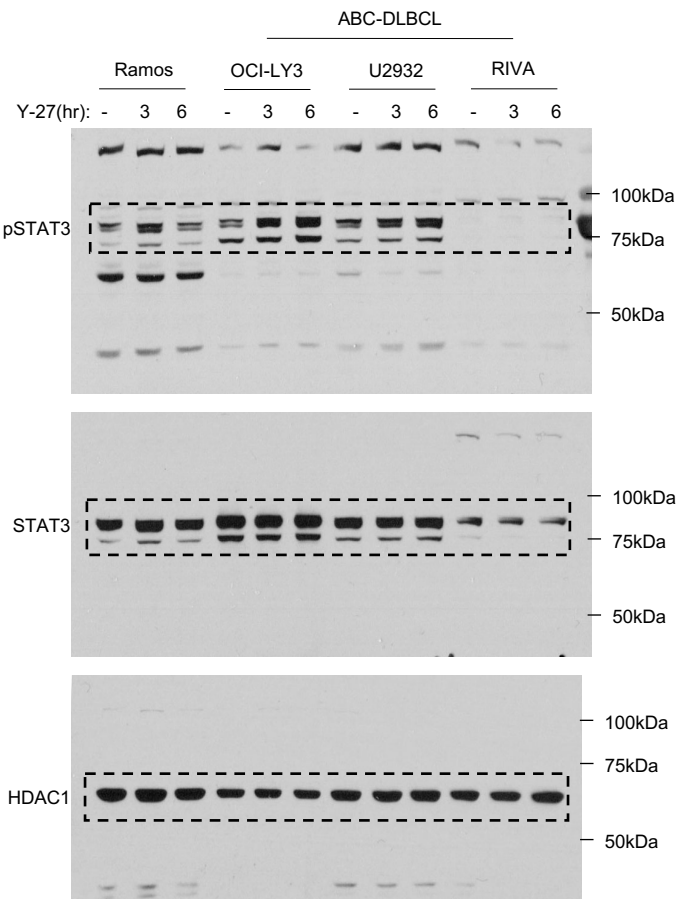


## Figure 1E

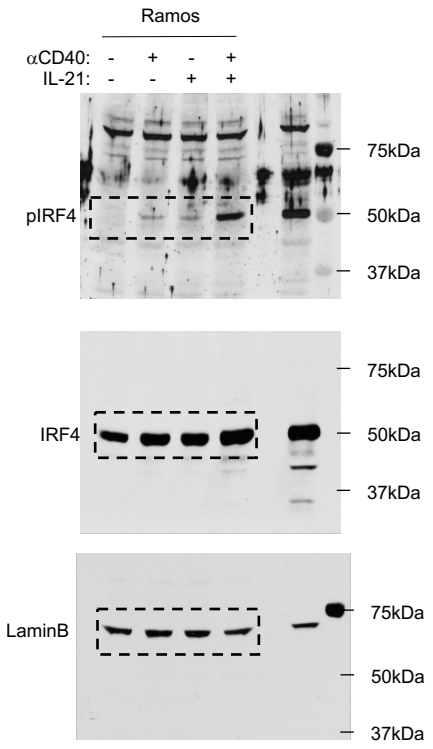
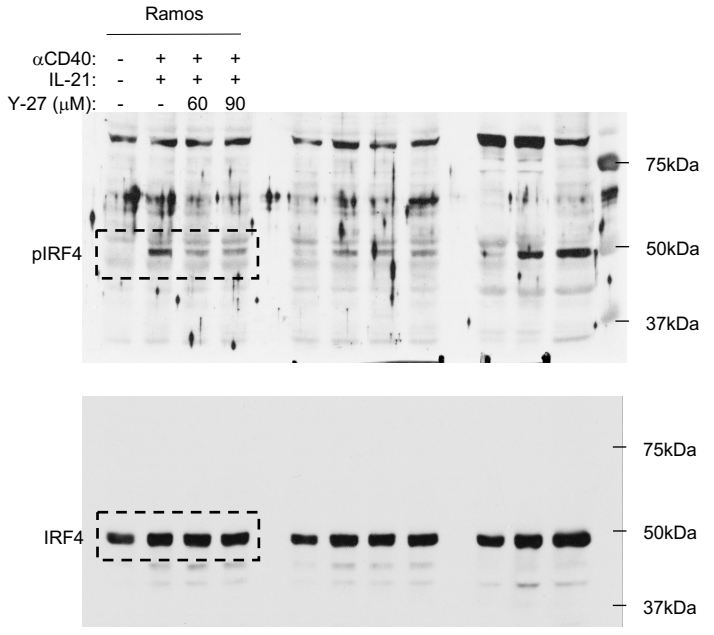


## Figure 1F



# Full Uncut Gels:

## Figure 1G

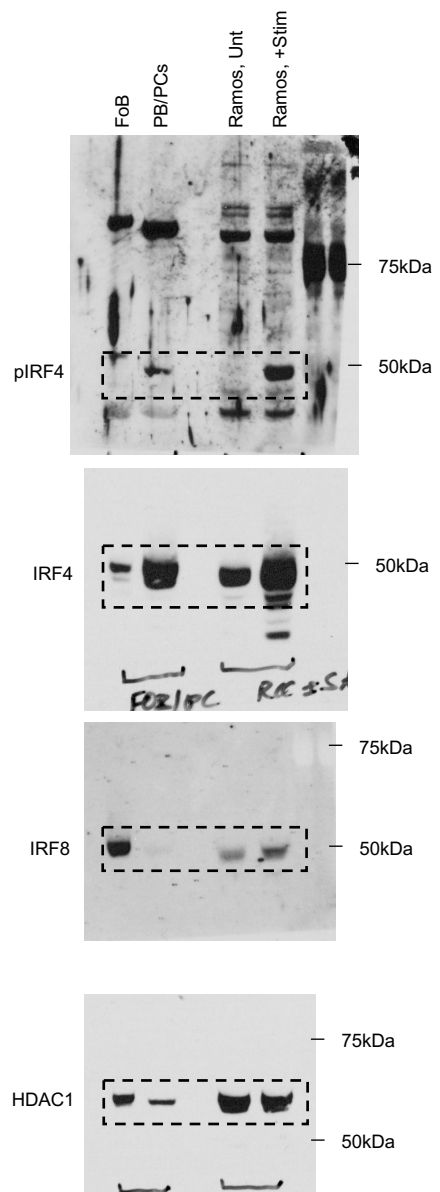


## Figure 2A

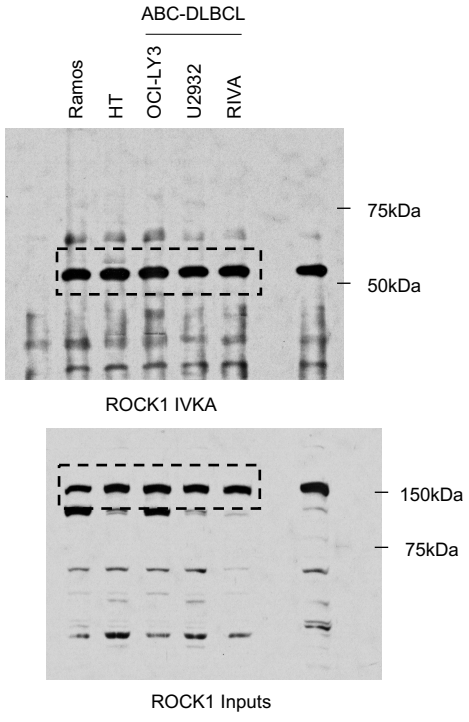
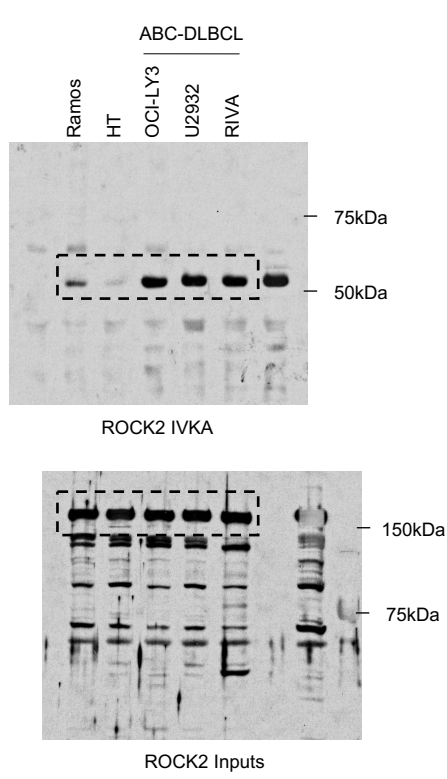


## Figure 2B



# Full Uncut Gels:

## Figure 2C

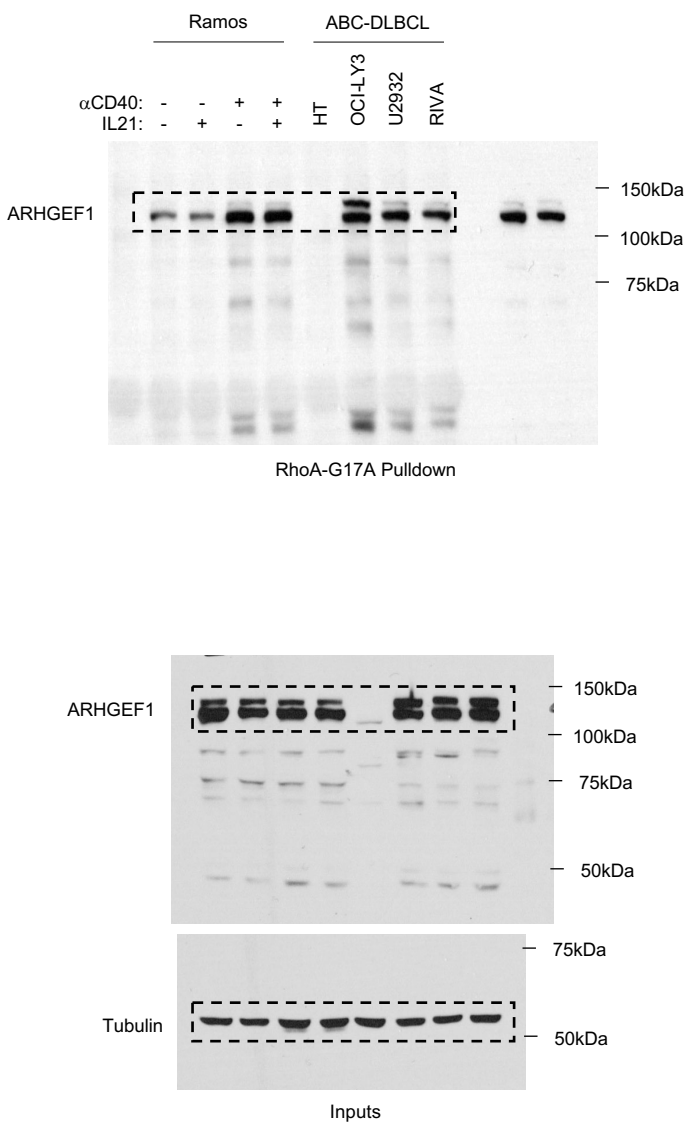
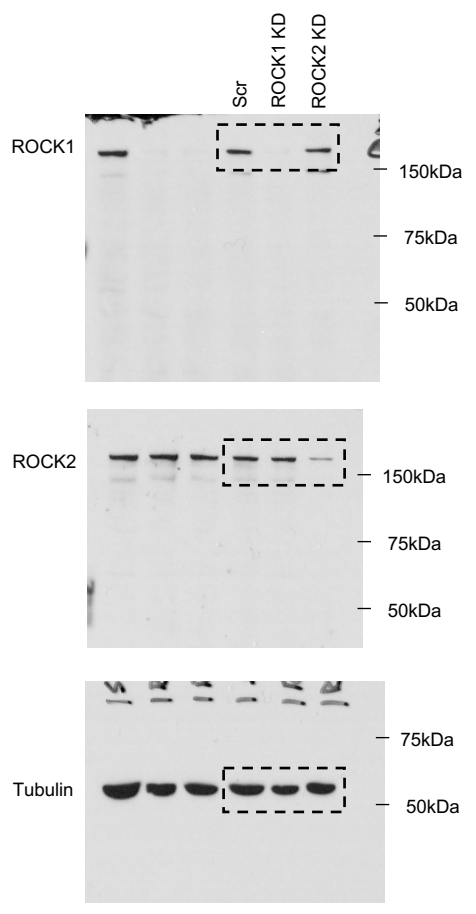


## Figure 3A





# Full Uncut Gels:

### Figure 3B

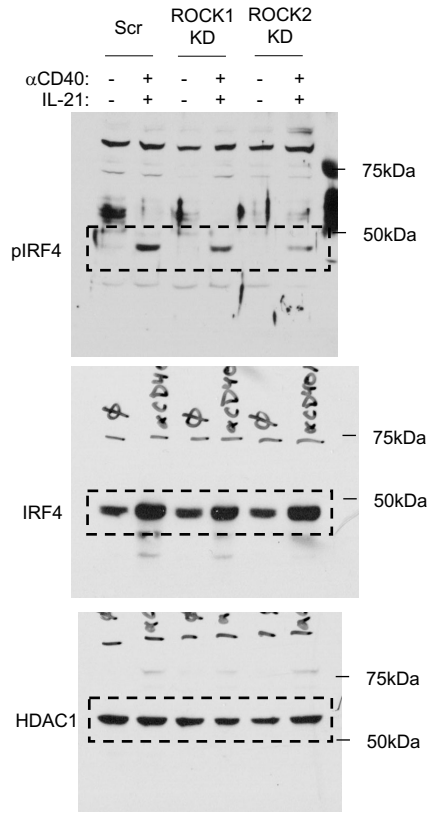


### Figure 3G

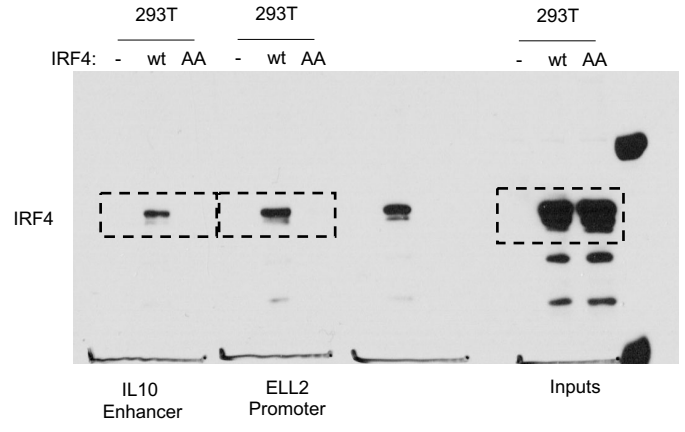
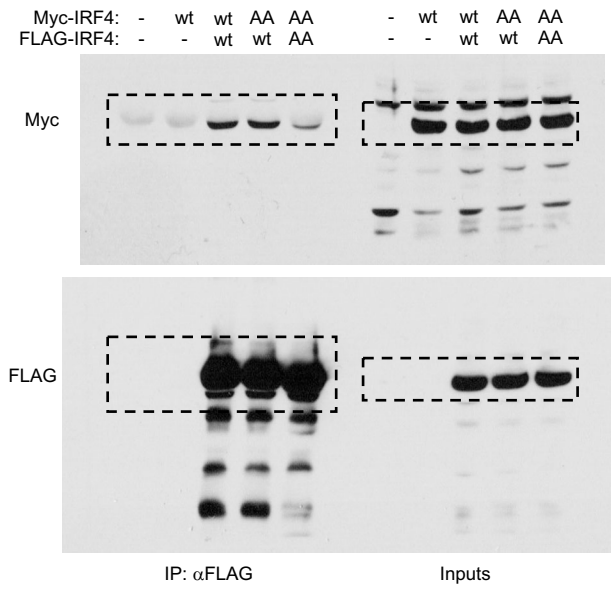


### Figure 3H



**Full Uncut Gels:**

**Figure 4A**

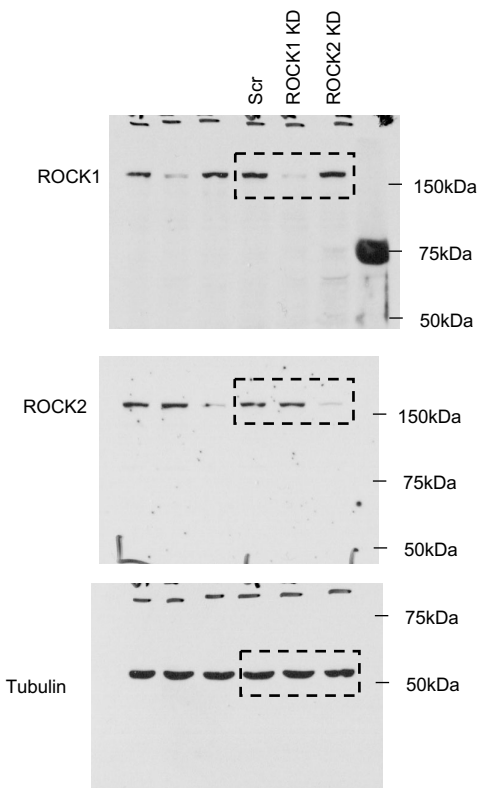


**Figure 5A**

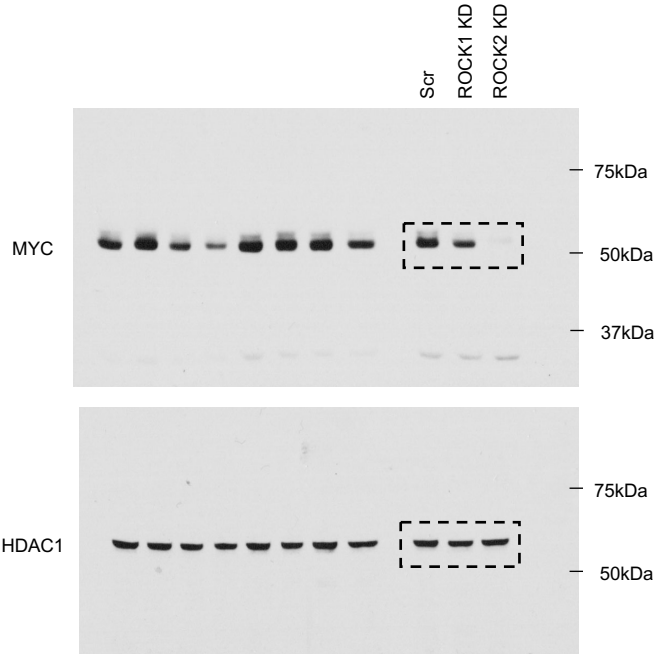


**Figure 4B**

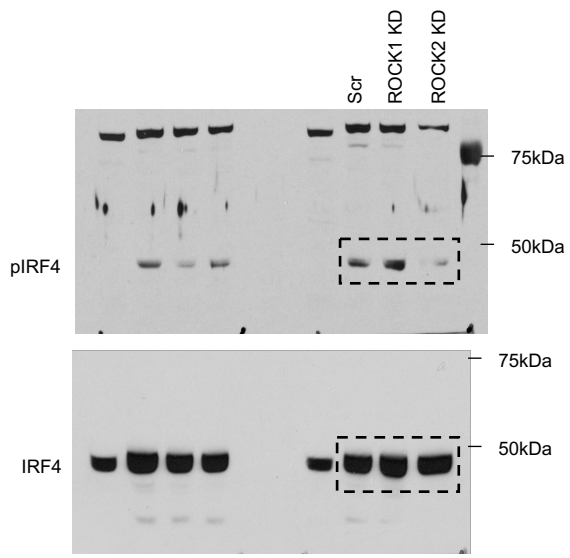
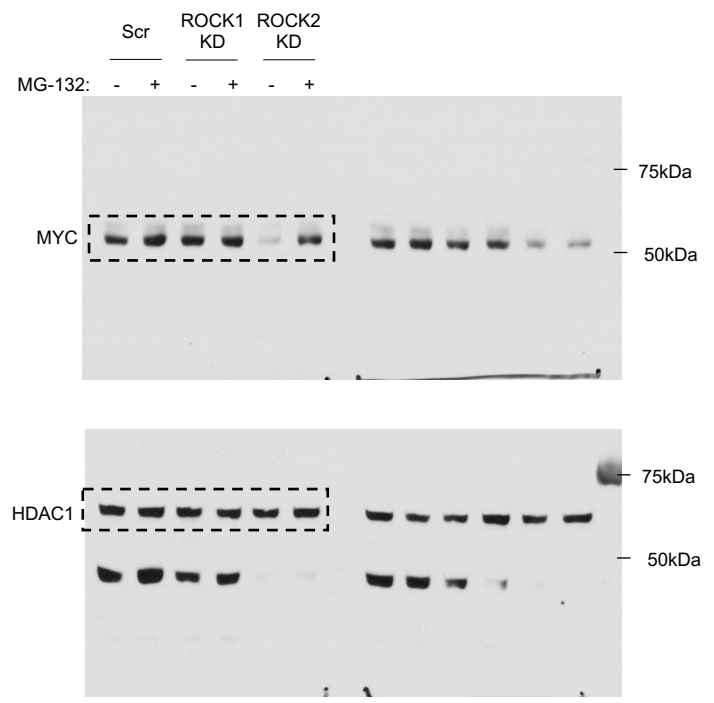


**Figure 5D**



**Full Uncut Gels:**

**Figure 5F**

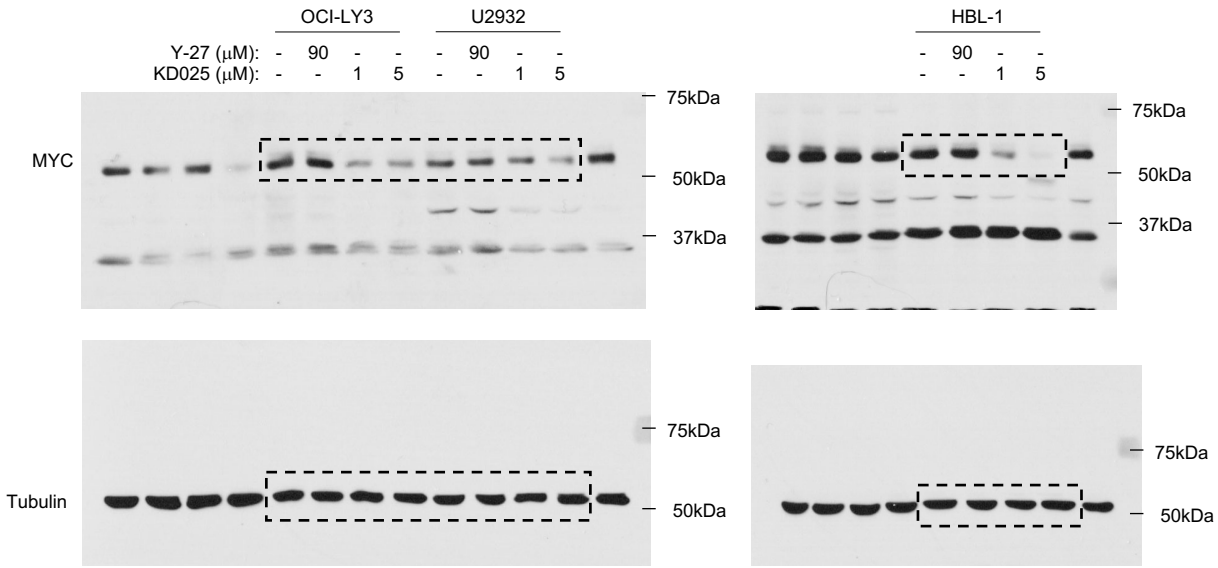
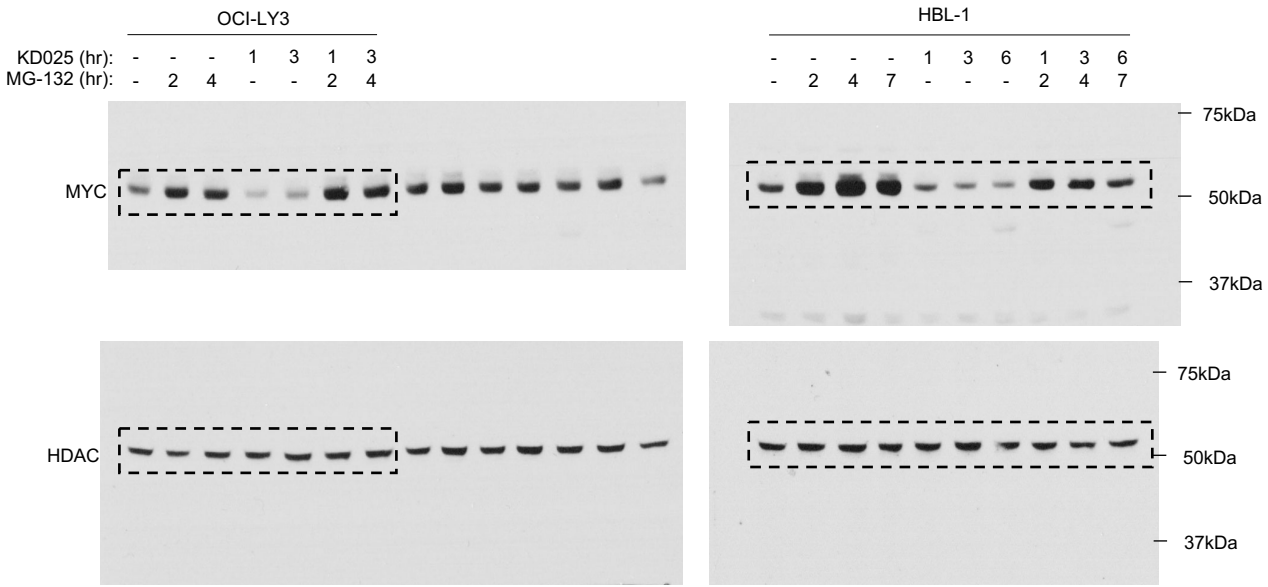


**Figure 5G**



# Full Uncut Gels:

## Figure S1A

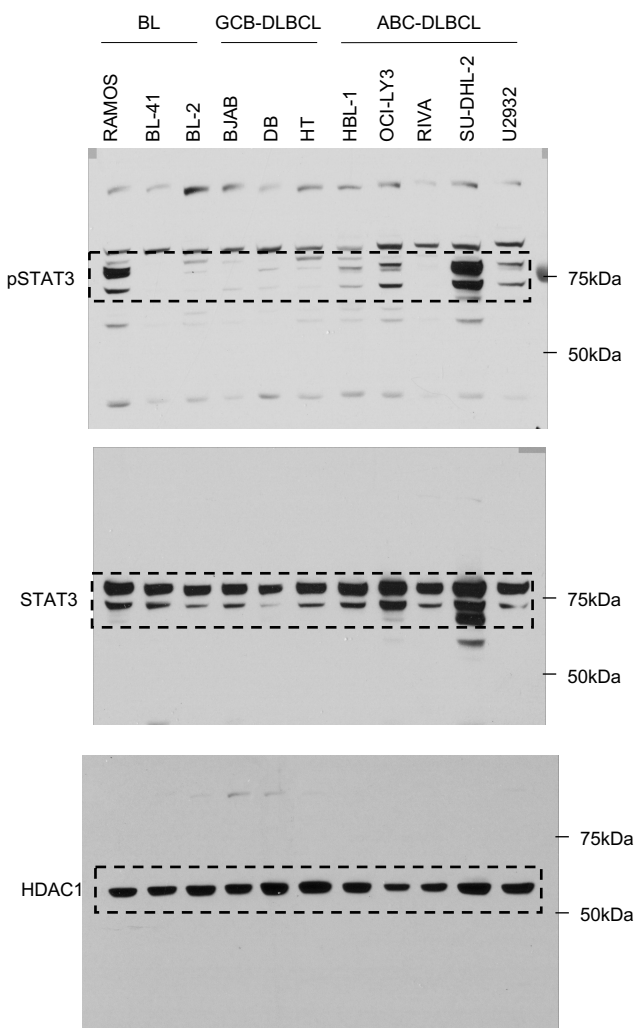
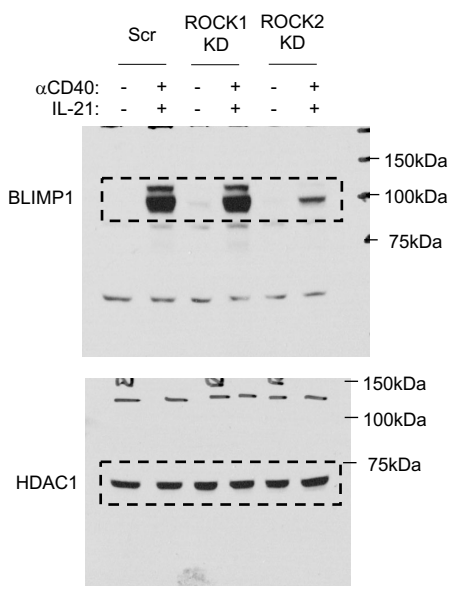


## Figure S2B



**Full Uncut Gels:**

**Figure S4E**

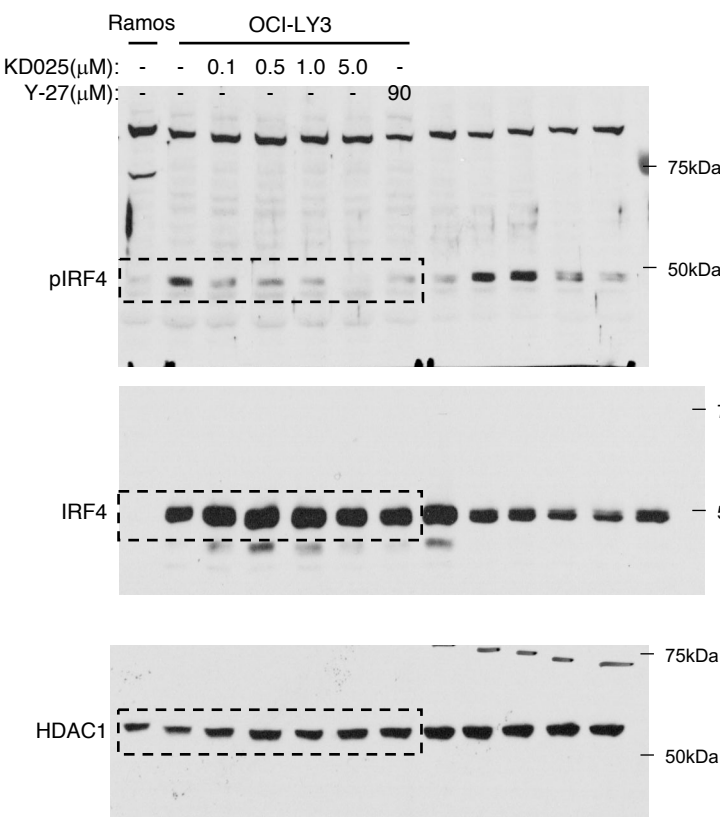
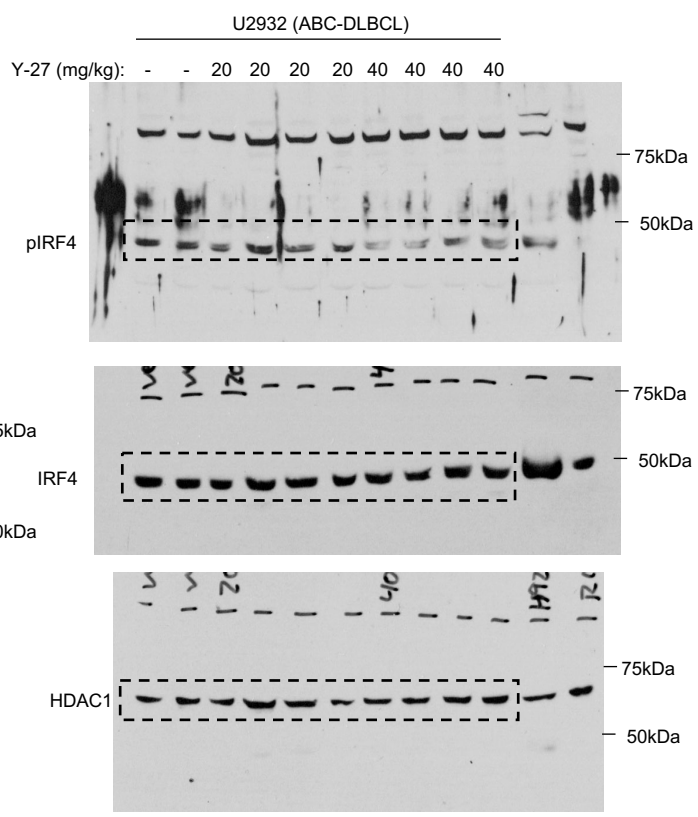
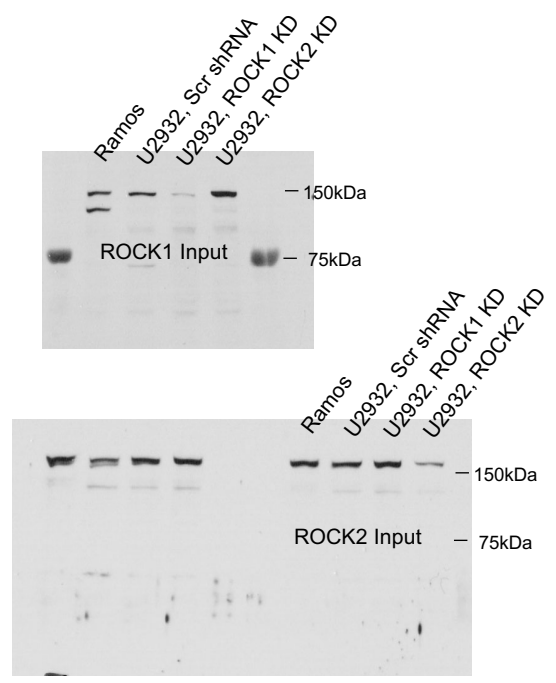
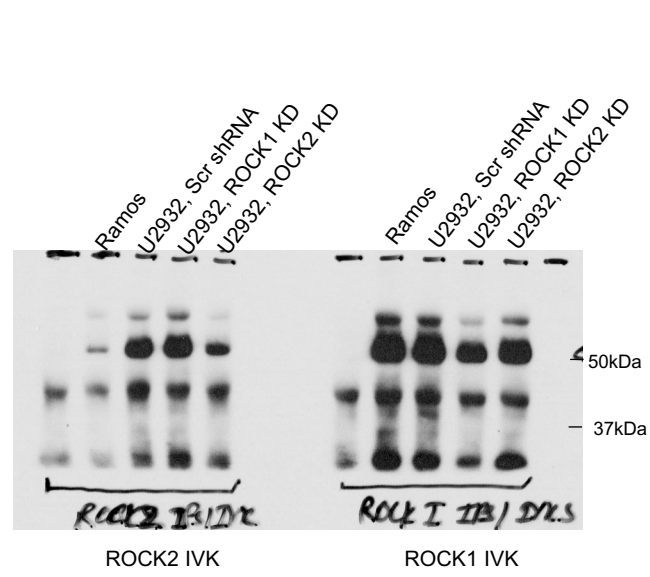


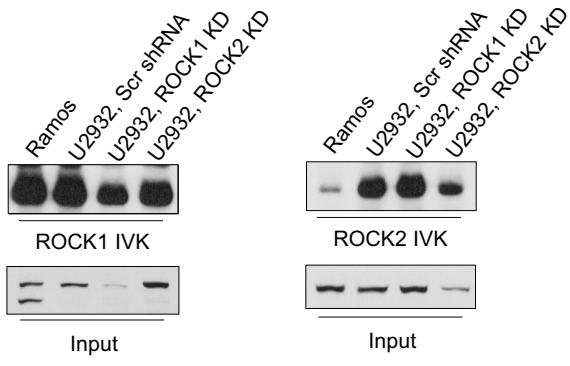
**Figure S6B**



**Data for Reviewers**



**Data for Reviewers.**



**Data for Reviewers.** ROCK1 and ROCK2 IVKs in U2932 cells following lentiviral knockdown of ROCK1, ROCK2, or following expression of a non-specific shRNA construct (Scr shRNA).